

Exploring Carbon Nanotubes/BaTiO₃/Fe₃O₄ Nanocomposites as Microwave Absorbers

Dzmitry Bychanok^{1, *}, Gleb Gorokhov¹, Darya Meisak¹, Artyom Plyushch¹, Polina Kuzhir^{1,2}, Alexey Sokal³, Konstantin Lapko³, Angela Sanchez-Sanchez⁴, Vanessa Fierro⁴, Alain Celzard⁴, Cameron Gallagher⁵, Alastair P. Hibbins⁵, Feodor Y. Ogrin⁵, and Christian Brosseau⁶

Abstract—We report the modelling and characterization of microwave absorbing materials specially designed for 26–37 GHz frequency range (Ka-band). Composite materials based on carbon nanotubes/BaTiO₃/Fe₃O₄ in a phosphate ceramic matrix were produced, and their electromagnetic response was investigated. Both theoretical and experimental results demonstrate that this material can absorb up to 100% of the power of an incident plane wave at a normal incidence angle. The physics underlying such absorption level is discussed in terms of refractive index of the material.

1. INTRODUCTION

The design and construction of compact multifunctional, thermally stable microwave radiation absorbers is technologically important for a number of applications. Of particular relevance is the development of the future generation communication systems, in which the questions of electromagnetic compatibility alongside the environmental protection will have to be addressed. There is a worldwide activity in this sector, and the search for new broadband absorbing materials is ongoing constantly [1–6]. The role of ferromagnetic resonance [7–9], Ohmic losses [10–12], dipole relaxation [13] and lossy scattering on the periodic structure of metamaterials [14] are some of the currently pursued questions. Some of these physical mechanisms can be efficiently combined in (nano)composite materials. A number of studies [15–20] showed that nano-sized inclusions can significantly affect the electromagnetic response of composites and provide an efficient way to tune their absorbing properties.

In the present work, the parameters of absorption of microwave radiation in composites based on a phosphate ceramic matrix [21, 22] were analysed. Our recent studies devoted to microwave absorbing materials [10] highlighted the main limitations of several physical parameters (complex effective permittivity, thickness, surface shape, etc.) for the design of effective nonmagnetic radar absorbers. Specifically, a 1 mm-thick single layer of a homogeneous material can absorb no more than 53% of the power of the incident radiation at 30 GHz. The only way of increasing the absorption level is by increasing the total thickness of the composite. This problem is especially important for aerospace applications, for which lightness and portability are crucial issues. The total thickness of the absorbing coating can be reduced when the composite is located on a metal plate (composite with

Received 11 May 2016, Accepted 11 July 2016, Scheduled 18 July 2016

* Corresponding author: Dzmitry Bychanok (dzmitrybychanok@ya.ru).

¹ Research Institute for Nuclear Problems Belarusian State University, 11 Bobruiskaya str., Minsk 220030, Belarus. ² Tomsk State University, Tomsk 634050, Russian Federation. ³ Research Institute for Physical Chemical Problems of the Belarusian State University, 14 Leningradskaya str., Minsk 220030, Belarus. ⁴ Institut Jean Lamour, UMR Université de Lorraine, CNRS 7198, ENSTIB, 27 rue Philippe Seguin, CS 60036, 88026 Epinal Cedex, France. ⁵ University of Exeter, Exeter EX4 4QL, United Kingdom. ⁶ Université Européenne de Bretagne, Université de Brest, Lab-STICC, CS 93837, 6 avenue Le Gorgeu, 29238 Brest Cedex 3, France.

a back reflector) [23]. Herein, we assume that the metal plate is a perfectly conducting layer with a reflection coefficient set to 1.

In Section 2, we develop a description of the reflection/absorption coefficients of a composite with back reflector and investigate their dependencies on several physical parameters. Next, in Section 3, we experimentally measure and discuss the frequency dependence of the absorption coefficient of composites based on multi-walled carbon nanotubes (MWCNTs)/BaTiO₃/Fe₃O₄ particles embedded in a phosphate ceramic matrix. Conclusions are given in Section 4.

2. EFFECTIVE ABSORBING COMPOSITE MODELLING

All the results below are given in the SI units, and we assume an $\exp[i(kz - \omega t)]$ dependence of the incident electric field. Let us consider the normal scattering of an incident plane wave on a plane-parallel layer of composite material located on a metal plate. The first-principles equations describing the electromagnetic response of such system in free space are well known [7, 24]. The amplitude of the reflected signal in the waveguide is defined as [10, 25]:

$$S_{11}(\lambda, \tau, n) = -\frac{k_z(\exp[2i\tau k_{2z}] - 1) + k_{2z}(1 + \exp[2i\tau k_{2z}])}{k_z(1 - \exp[2i\tau k_{2z}]) + k_{2z}(1 + \exp[2i\tau k_{2z}])}, \quad (1)$$

with

$$k_z = \frac{\pi}{\lambda a} \sqrt{4a^2 - \lambda^2}, \quad k_{2z} = \frac{\pi}{\lambda a} \sqrt{4n^2 a^2 - \lambda^2}, \quad n = \sqrt{\varepsilon\mu}, \quad (2)$$

where τ is the thickness of the composite, a the width of the waveguide (set to 7.2 mm), $\lambda = c/\nu$ the wavelength, c the vacuum light velocity, ν the frequency, $n = n' + in''$ the relative refractive index, ε the complex (relative) permittivity and μ the (relative) magnetic permeability of the composite. Eq. (1) can also be used in free space; in this case, wave vectors $k_z = 2\pi/\lambda$ and $k_{2z} = 2\pi n/\lambda$ should be used. From Eq. (1), it is easy to calculate the absorption coefficient as $A = 1 - |S_{11}|^2$.

To achieve maximum of the absorption, one can vary the composite thickness. Additionally, by changing the type of the filler and its content, it is also possible to change the refractive index to obtain the maximal absorption at fixed thicknesses and frequency. Fig. 1(a) shows a general view of the dependence of the absorption coefficient $A = 1 - |S_{11}|^2$ on the real and imaginary parts of the refractive index, calculated using Eq. (1) for a 0.65 mm-thick composite attached to a metal plate at 30 GHz. The corresponding cross-sections of this three-dimensional plot around the maximum are displayed in Figs. 1(b)–(c).

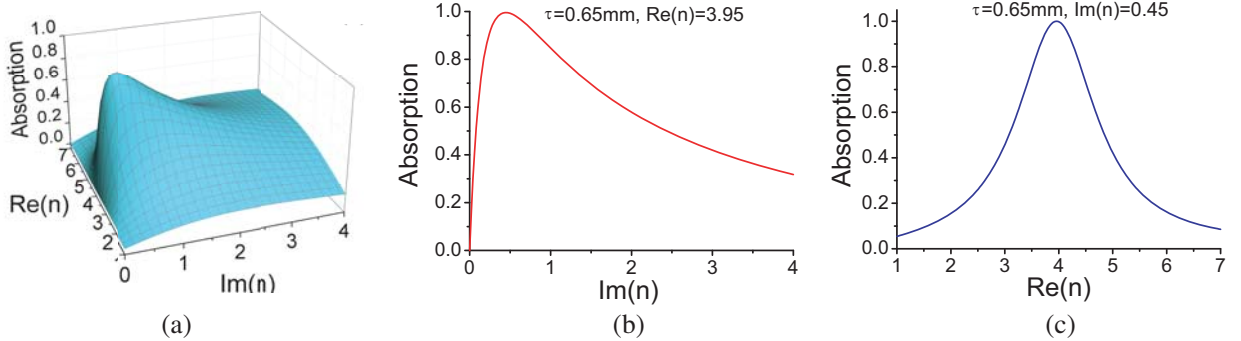


Figure 1. (a) Dependence of the absorption coefficient A on the real and imaginary parts of the refractive index of a 0.65 mm-thick composite located on a metal plate at 30 GHz in the waveguide; (b) Cross-section of (a) versus $\text{Im}(n)$ for $\text{Re}(n) = 3.95$; (c) Cross-section of (a) versus $\text{Re}(n)$ for $\text{Im}(n) = 0.45$.

In Fig. 1, only the first absorption maximum, related to minimal values of $\text{Re}(n)$, was presented as it is the most important for practical applications. As shown in Fig. 1, the maximum of the absorption may reach up to 100% near the point of $n = 3.95 + i0.45$. It can be seen for both cases, in free space and inside the waveguide. The dependence of its position on the thickness and the frequency

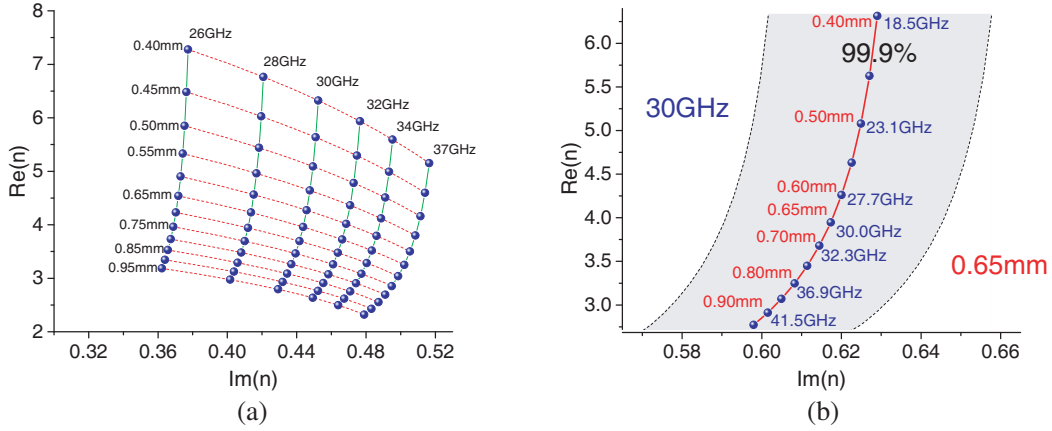


Figure 2. Maximum of absorption as function of thickness and frequency inside (a) the waveguide and (b) in free space.

inside the waveguide is shown in Fig. 2(a). In this figure, these two parameters are varied in the range 0.40–0.95 mm and 26–37 GHz, respectively, and the positions of corresponding absorption maxima are estimated.

The dependence of the absorption maximum on the thickness at constant frequency in the waveguide is presented in Fig. 2(a) with green solid lines. One can see that an increase of thickness leads to a monotonic shift of the maximum position to lower values of $Re(n)$ and $Im(n)$. Nevertheless the position of $Im(n)$ coordinate is less sensitive to the variation of τ , especially at low frequencies. From Fig. 2(a) it is obvious, that in order to achieve the same absorption at lower thicknesses, the materials with higher values of refractive index should be used. The dependence of the position of the absorption maximum on the frequency at constant thickness in the waveguide is presented in Fig. 2(a) with dashed red lines. It can be seen that by increasing the frequency the maximum of the absorption peak is shifted to lower values of $Re(n)$ and to higher values of $Im(n)$. This demonstrates an effective way of using dispersive materials to obtain a broadband absorption.

For the case of absorption in free space, Eq. (1) can be significantly simplified and the coordinates of the absorption maximum can be obtained as roots of the following transcendental equation

$$\tan(2\pi\nu\tau n/c) = in. \tag{3}$$

This equation depends only on the product of thickness τ and frequency ν . So the variation of both parameters in free space are equivalent and, in contrast to Fig. 2(a), all roots are located on one curve presented in Fig. 2(b) with solid red line. In this figure we fixed the frequency at 30 GHz and varied the thickness (red labels) to find the corresponding absorption peak positions (blue dots) and then vice-versa we fixed the thickness at 0.65 mm and estimated the frequency at the same peak positions (blue labels). Additionally, for practical use, we highlighted by grey colour the region near the red curve, where absorption is $> 99.9\%$. If the refractive index of non-dispersive material is located in the grey region of Fig. 2(b), it is always possible to find the required thickness of the material to obtain the maximum absorption at a given frequency. Analysis of Fig. 2(b) shows that an increase in the frequency leads to a similar monotonic shift of the maximum absorption peak to lower values of $Re(n)$ and $Im(n)$. Nevertheless, the variation of thickness and frequency generally affects the $Re(n)$ coordinate of the absorption peak. $Im(n)$ is less sensitive to changes of frequency and thickness (e.g., in Fig. 2(b) $Re(n)$ related to red curve is varied in the range 6.31–2.77, and $Im(n)$ is varied in the range 0.60–0.63). So the materials with $Im(n) = 0.60\text{--}0.63$ are expected to have good absorbing properties in Ka-band.

It is worth noticing that in free space the same absorption peak for 0.65 mm-thick composite as in Fig. 1 is located at higher values of $Im(n)$ (Fig. 3) and practically at the same value of $Re(n) = 3.95$. This is due to the wave vector difference in free space ($k_z = 2\pi/\lambda, k_{2z} = 2\pi n/\lambda$) and in the waveguide ($k_z = \frac{\pi}{\lambda a} \sqrt{4a^2 - \lambda^2}, k_{2z} = \frac{\pi}{\lambda a} \sqrt{4n^2 a^2 - \lambda^2}$). Consequently, a good absorber inside the waveguide is not adapted for free space and should be modified by changing either the filler content or by varying the filler type in the composite material. In the following work, adding multi-walled CNTs (MWCNTs) to

the composite material was suggested in order to increase $\text{Im}(n)$. Even low CNT amounts (< 5 wt.%) indeed drastically affect the electromagnetic properties of a neat polymer matrix [17, 18]. Hence, by varying the MWCNT content, it is possible to obtain a highly absorbing material in free space (Fig. 3). The specific MWCNT content to achieve refractive index for maximal absorption can be well predicted and controlled by use of the Maxwell Garnett mixing law [12, 18] or the Bruggeman effective equation.

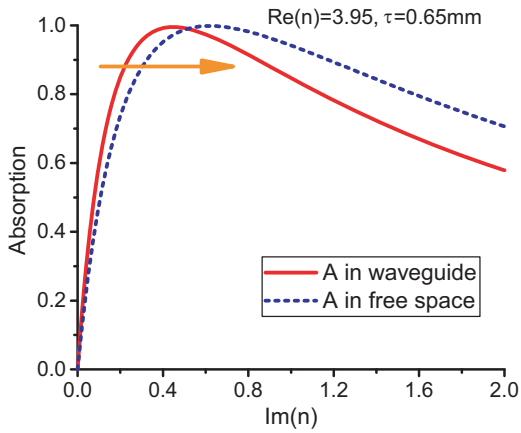


Figure 3. Dependence of the absorption coefficient A on the imaginary part of the refractive index of a 0.65 mm-thick composite located on a metal plate at 30 GHz in the waveguide and in free space ($\text{Re}(n)$ is fixed and set to 3.95).

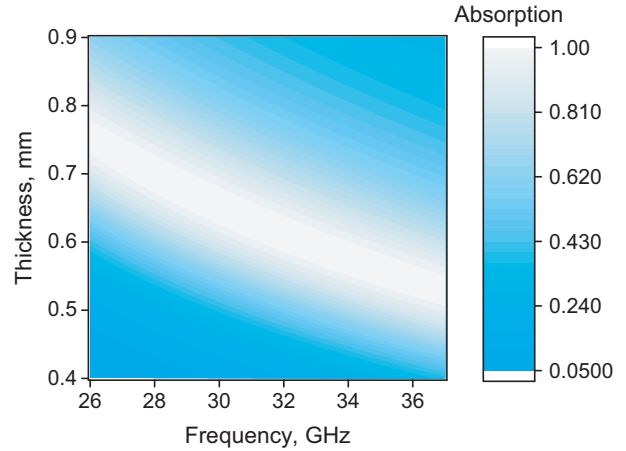


Figure 4. Dependence of the absorption coefficient A on frequency and thickness of a composite with $n = 3.95 + i0.45$ located on a metal plate in the waveguide.

In practice, when the frequency range is fixed, the maximum of absorption is estimated, and once the corresponding composite material is produced, it is very useful to investigate the frequency dependence of the absorption coefficient of samples with various thicknesses. Fig. 4 shows a two-dimensional density plot of the absorption coefficient obtained by varying both frequency and thickness for a composite with $n = 3.95 + i0.45$ inside the waveguide.

From Fig. 4, it can be seen that the maximum of absorption is shifted to higher frequencies when the thickness of the composite is decreased.

3. RESULTS AND DISCUSSION

3.1. Sample Preparation

Composite materials with a refractive index close to the maximum of absorption displayed in Fig. 1 can be fabricated by mixing magnetic particles (magnetite Fe_3O_4), piezoelectric particles (barium titanate BaTiO_3), and carbon nanotubes in a phosphate ceramic matrix. Similar multiferroic composites made by combining piezoelectric and magnetostrictive nanoparticles were already investigated in the GHz range of frequencies [26]. The composites were produced as described in [21]. In the present study, commercially available (Aldrich) magnetite Fe_3O_4 nanoparticles of mean size 50–100 nm, piezoelectric (Aldrich) BaTiO_3 nanoparticles (cubic) of mean size 50 nm, and phosphate matrix [21] in equal mass proportions were used. For tuning the refractive index of such 3-phase mixture, 0.1 wt.% of MWCNT [27] was also added. The components were mixed together and pressed in tablets under a pressure of 20 MPa. After 12 h curing in air at room temperature, the samples were heat treated in an oven to 200°C. Samples used for microwave characterization were prepared as parallelepipeds of width 3.4 mm, length 7.2 mm, and various thicknesses (Fig. 5(a)).



Figure 5. (a) General view of prepared composites without MWCNTs (left) and with 0.1 wt.% of MWCNTs (right); (b) Scalar network analyser ELMIKA R2-408R used for Ka-band measurements.

3.2. Ka-Band Measurements

Microwave measurements were carried out using a scalar network analyser ELMIKA R2-408R (Fig. 5(b)). All measurements were performed in a 7.2×3.4 mm waveguide system. In a typical experiment, the plane-parallel layer of the composite was placed normally to the wave vector of the incident radiation. Behind the sample was located the short end (i.e., the mirror with a reflection coefficient of 100%). The scattering coefficient S_{11} of the sample was obtained as the ratio of the reflected amplitude signal to the input one. The spectral variation of the S-parameter of the 0.65 mm-thick composite without MWCNT addition is presented in Fig. 6. It can be seen that these data are well matched by Eq. (1) with the parameter $n = 3.95 + i0.45$ (solid line in Fig. 6). As depicted in Fig. 6, the absorption coefficient $A = 1 - |S_{11}|^2$ around 30 GHz is close to 100% and the refractive index of the $\text{Fe}_3\text{O}_4/\text{BaTiO}_3/\text{phosphate}$ composite is close to the maximum of absorption shown in Fig. 1. Within the whole frequency range 26–37 GHz, the absorption varied from 65 to 100%.

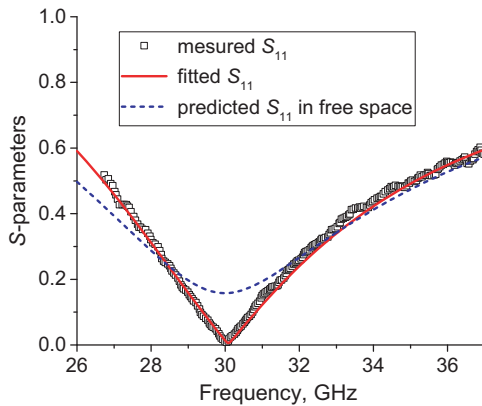


Figure 6. Frequency dependence of measured S_{11} -parameters of a 0.65 mm-thick composite in the waveguide (squares). The solid (red) line is a fit to the data using Eq. (1) with $n = 3.95 + i0.45$. The dashed (blue) line represents the predicted S_{11} -parameters of a 0.65 mm-thick composite in free space.

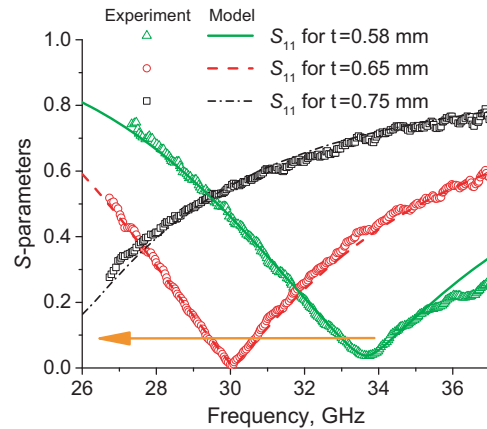


Figure 7. Frequency dependence of the measured (data points) and fitted (lines) S_{11} -parameters of 0.75, 0.65 and 0.58 mm-thick composites in the waveguide. The arrow corresponds to the growth of the thickness.

Additionally, the maximum of absorption could be easily varied by changing the sample thickness. The experimentally measured S -parameters of samples with various thicknesses are presented in Fig. 7, as well as their fits by Eq. (1) using $n = 3.95 + i0.45$. These data are consistent with those of Fig. 4, i.e., the decrease of the thickness produces a shift of the maximum of absorption to higher frequencies.

3.3. Using MWCNTs for Free Space Applications

Using Eq. (1) with $k_z = 2\pi/\lambda$ and $k_{2z} = 2\pi n/\lambda$, the free space electromagnetic response of composites located on a metal plate can be estimated. The data for a 0.65 mm-thick composite with $n = 3.95 + i0.45$ are presented in Fig. 6 (dashed line). As depicted in Fig. 6, the free space absorption coefficient remains quite large but differs significantly from 100%. This result is consistent with the behavior shown in Fig. 3. Due to the difference of wave vector in free space and in the waveguide, higher values of the imaginary part of the refractive index are needed. For this purpose, the addition of MWCNTs in the composite sample can significantly change its electromagnetic properties. This is consistent with many previous investigations [17,18], and provides a simple way to reach the maximum absorption in free space using this type of ceramics. In practice, we found by successive trials that adding a small amount of MWCNTs allows us to reach a value of $\text{Im}(n)$ inside the grey region of Fig. 2(b). By adding small amount below the percolation threshold of MWCNTs in the composite sample, both imaginary and real parts of the refractive index can be increased. This is due to MWCNTs high values of real and imaginary parts of polarizability [28]. Due to the high sensitivity of $\text{Re}(n)$ -coordinate of the absorption maximum to the change of thickness compared to that of $\text{Im}(n)$ -coordinate, the region near the maximum of absorption can be approached again, when the composite thickness is decreased. The measured frequency dependence of S_{11} for the 0.55 mm-thick composite containing 0.1 wt.% of MWCNTs located on a metal plate is presented in Fig. 8. The data were satisfactorily fitted with Eq. (1) with $n = 4.70 + i0.61$ (solid line in Fig. 8). It can be seen that the absorption coefficient in free space is very close to 100% around 30 GHz (dashed line in Fig. 8).

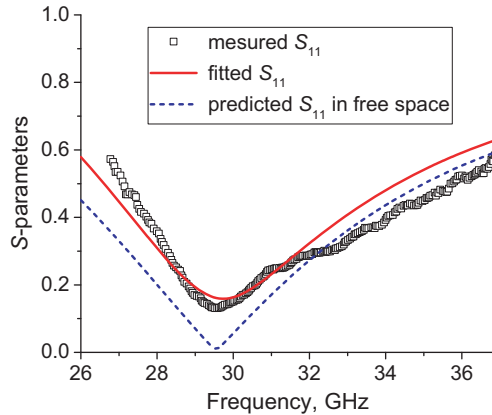


Figure 8. Frequency dependence of the measured S_{11} -parameters of a 0.55 mm-thick composite in the waveguide (squares). The solid (red) line is a fit to the data using Eq. (1) with $n = 4.70 + i0.61$. The dashed (blue) line represents the predicted S_{11} -parameters of a 0.55 mm-thick composite in free space.

Figure 8 shows that MWCNTs addition to the ceramic matrix allowed a significant improvement of the absorption in free space. As discussed above, the higher value of the refractive index led to a decrease of the composite thickness from 0.65 to 0.55 mm for the maximum of absorption around 30 GHz.

3.4. Further Practical Application

The demonstrated results can be found practical for developing microwave absorbers operating at a fixed frequency. We showed that in the range of 26–37 GHz the absorption level varied from 65 to 100%. It is worth noting that our results are scalable and that their validity can be extended to other frequency ranges. Additionally, the ceramics under study are inert and thermally stable so these materials may potentially be used for high-power absorbers. Analysis of Eq. (1) provides a simple way of estimating the effective refractive index of the material with the maximum of the absorption at specified frequency and thickness (Fig. 2). Equally it can be used to find the necessary thickness of the material with the given electromagnetic parameters (Fig. 4).

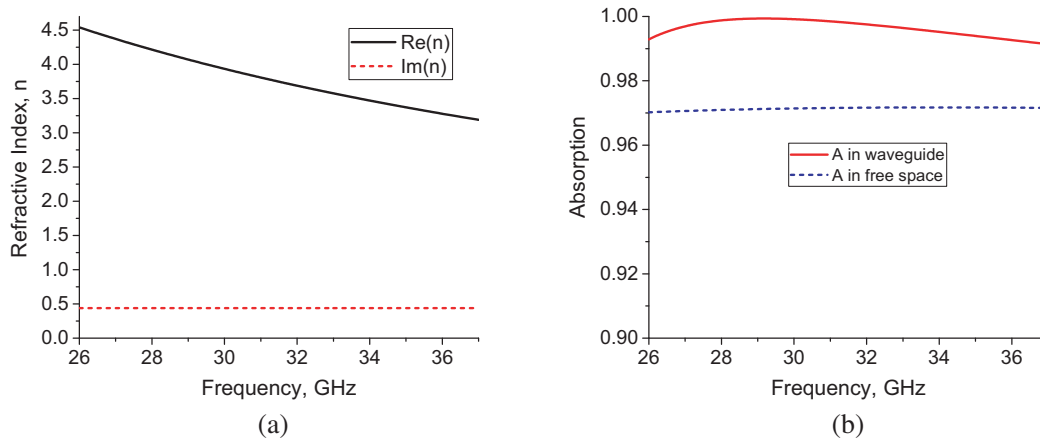


Figure 9. (a) Frequency dependence of the refractive index n for broadband absorption; (b) Frequency dependence of absorption coefficient A of a 0.65 mm-thick composite with $n(\nu)$ located on the metal plate in the waveguide and in free space.

It is also important to note that these results are relevant to monochromatic wave absorption. To obtain broadband absorption, dispersive materials are needed (Fig. 2). For example, because of the $\simeq 1/\nu$ frequency dependence [7] of the real part of the refractive index (Fig. 9(a)), the absorption peak in Fig. 1 can be broad, and it is theoretically possible to absorb more than 97% of the initial radiation power in the whole Ka-band (Fig. 9(b)). Another interesting candidate for effective absorbers with refractive index similar to the one displayed in Fig. 9 is based on a phosphate ceramic matrix loaded with MWCNTs content above the percolation threshold [21].

4. CONCLUSION

The presented results demonstrate a good potential for constructing surfaces absorbing 100% of the incident microwave radiation in a waveguide and in free space. Since the materials under study are thermally stable, thin, cost-effective and easy-to-produce, they have important potentialities for aerospace technologies. The highly absorbing region was found around the interference minimum. Within the 26–37 GHz frequency range, the absorption level varied from 65 to 100%. The maximum of the absorption of the sample could be shifted by varying the sample thickness. Addition of a small amount (below percolation) of MWCNTs to the ceramic allowed tuning the refractive index of the composite for specific civilian and military applications.

ACKNOWLEDGMENT

This work was supported in part by FP7-PEOPLE-2013-IRSES-610875 NAmiceMC, FP7 Twinning Grant Inconet EaP_004. P. Kuzhir is thankful for support by Tomsk State University Competitiveness Improvement Program. Lab-STICC is UMR CNRS 6285.

REFERENCES

1. Qiang, C., J. Xu, Z. Zhang, L. Tian, S. Xiao, Y. Liu, and P. Xu, "Magnetic properties and microwave absorption properties of carbon fibers coated by Fe_3O_4 nanoparticles," *Journal of Alloys and Compounds*, Vol. 506, 93–97, 2010.
2. Tsay, C. Y., R. B. Yang, D. S. Hung, Y. H. Hung, Y. D. Yao, and C. K. Lin, "Investigation on electromagnetic and microwave absorbing properties of $\text{La}_{0.7}\text{Sr}_{0.3}\text{MnO}_3$ -d/carbon nanotube composites," *Journal of Applied Physics*, Vol. 107, 09A502, 2010.

3. Danlee, Y., I. Huynen, and C. Bailly, "Thin smart multilayer microwave absorber based on hybrid structure of polymer and carbon nanotubes," *Applied Physics Letters*, Vol. 100, 213105, 2012.
4. Duan, M. C., L. M. Yu, L. M. Sheng, K. An, W. Ren, and X. L. Zhao, "Electromagnetic and microwave absorbing properties of SmCo coated single-wall carbon nanotubes/NiZn-ferrite nanocrystalline composite," *Journal of Applied Physics*, Vol. 115, 174101, 2014.
5. Kim, S.-T. and S.-S. Kim, "Microwave absorbing properties of hollow microspheres plated with magnetic metal films," *Journal of Applied Physics*, Vol. 115, 17A528, 2014.
6. El-Hakim, H. A., K. R. Mahmoud, and A. Abdelaziz, "Design of compact double-layer microwave absorber for X-Ku bands using genetic algorithm," *Progress In Electromagnetics Research B*, Vol. 65, 157–168, 2016.
7. Zhuravlev, V., V. Suslyayev, E. Korovin, and K. Dorozhkin, "Electromagnetic waves absorbing characteristics of composite material containing carbonyl iron particles," *Materials Sciences and Applications*, Vol. 5, 803–811, 2014.
8. Ipatov, M., V. Zhukova, L. V. Panina, and A. Zhukov, "Ferromagnetic microwires composite metamaterials with tuneable microwave electromagnetic parameters," *PIERS Proceedings*, Vol. 5, 586–590, Beijing, China, March 23–27, 2009.
9. Zivkovic, I. and A. Murk, "Characterization of magnetically loaded microwave absorbers," *Progress In Electromagnetics Research B*, Vol. 33, 277–289, 2011.
10. Bychanok, D., S. Li, A. Sanchez-Sanchez, G. Gorokhov, P. Kuzhir, F. Ogrin, A. Pasc, T. Ballweg, K. Mandel, A. Szczurek, V. Fierro, and A. Celzard, "Hollow carbon spheres in microwaves: Bio-inspired absorbing coating," *Applied Physics Letters*, Vol. 108, 013701, 2016.
11. Cao, M.-S., W.-L. Song, Z.-L. Hou, B. Wen, and J. Yuan, "The effects of temperature and frequency on the dielectric properties, electromagnetic interference shielding and microwave-absorption of short carbon fiber/silica composites," *Carbon*, Vol. 48, 788–796, 2010.
12. Sarto, M. S., A. G. D'Aloia, A. Tamburrano, and G. De Bellis, "Synthesis, modeling, and experimental characterization of graphite nanoplatelet-based composites for EMC applications," *IEEE Transactions on Electromagnetic Compatibility*, Vol. 54, 17–27, 2012.
13. Buchner, R., J. Barthel, and J. Stauber, "The dielectric relaxation of water between 0°C and 35°C," *Chemical Physics Letters*, Vol. 306, 57–63, 1999.
14. Withayachumnankul, W. and D. Abbott, "Metamaterials in the terahertz regime," *Photonics Journal*, Vol. 1, 99–118, 2009.
15. Qin, F. and C. Brosseau, "A review and analysis of microwave absorption in polymer composites filled with carbonaceous particles," *Journal of Applied Physics*, Vol. 111, 061301–24, 2012.
16. Brosseau, C., P. Molinie, F. Boulic, and F. Carmona, "Mesostructure, electron paramagnetic resonance, and magnetic properties of polymer carbon black composites," *Journal of Applied Physics*, Vol. 89, 8297–8310, 2001.
17. Bychanok, D., P. Kuzhir, S. Maksimenko, S. Bellucci, and C. Brosseau, "Characterizing epoxy composites filled with carbonaceous nanoparticles from dc to microwave," *Journal of Applied Physics*, Vol. 113, 124103–6, 2013.
18. Kuzhir, P., A. Paddubskaya, D. Bychanok, A. Nemilentsau, M. Shuba, A. Plusch, S. Maksimenko, S. Bellucci, L. Coderoni, F. Micciulla, I. Sacco, G. Rinaldi, J. Macutkevic, D. Seliuta, G. Valusis, and J. Banys, "Microwave probing of nanocarbon based epoxy resin composite films: Toward electromagnetic shielding," *Thin Solid Films, Carbon- or Nitrogen-containing Nanostructured Composite Films*, Vol. 519, 4114–4118, 2011.
19. Apanasevich, N., A. Sokal, K. Lapko, A. Kudlash, V. Lomonosov, A. Plyushch, P. Kuzhir, J. Macutkevic, J. Banys, and A. Okotrub, "Phosphate ceramics — Carbon nanotubes composites: Liquid aluminum phosphate vs solid magnesium phosphate binder," *Ceramics International*, Vol. 41, 12147–12152, 2015.
20. Kanygin, M. A., O. V. Sedelnikova, I. P. Asanov, L. G. Bulusheva, A. V. Okotrub, P. P. Kuzhir, A. O. Plyushch, S. A. Maksimenko, K. N. Lapko, A. A. Sokol, O. A. Ivashkevich, and P. Lambin, "Effect of nitrogen doping on the electromagnetic properties of carbon nanotube-based composites," *Journal of Applied Physics*, Vol. 113, 144315, 2013.

21. Plyushch, A., D. Bychanok, P. Kuzhir, S. Maksimenko, K. Lapko, A. Sokol, J. Macutkevici, J. Banys, F. Micciulla, A. Cataldo, and S. Bellucci, "Heat-resistant unfired phosphate ceramics with carbon nanotubes for electromagnetic application," *Phys. Status Solidi A*, Vol. 211, 2580–2585, 2014.
22. Plyushch, A. O., A. A. Sokol, K. N. Lapko, P. P. Kuzhir, Y. V. Fedoseeva, A. I. Romanenko, O. B. Anikeeva, L. G. Bulusheva, and A. V. Okotrub, "Electromagnetic properties of phosphate composite materials with boron-containing carbon nanotubes," *Physics of the Solid State*, Vol. 56, 2537–2542, 2014.
23. Gaylor, K., "Radar absorbing materials-mechanisms and materials," *Materials Research Labs Ascot Vale (Australia)*, No. MRL-TR-89-1, 1989.
24. Baker-Jarvis, J., M. Janezic, J. J. Grosvenor, and R. Geyer, "Transmission/reflection and short-circuit line methods for measuring permittivity and permeability," *NIST Technical Note*, 1355, 1993.
25. Bychanok, D., A. Plyushch, K. Piasotski, A. Paddubskaya, S. Voronovich, P. Kuzhir, S. Baturkin, A. Klochkov, E. Korovin, M. Letellier, S. Schaefer, A. Szczurek, V. Fierro, and A. Celzard, "Electromagnetic properties of polyurethane template-based carbon foams in Ka-band," *Physica Scripta*, Vol. 90, 094019, 2015.
26. Castel, V. and C. Brosseau, "Magnetic field dependence of the effective permittivity in BaTiO₃/Ni nanocomposites observed via microwave spectroscopy," *Applied Physics Letters*, Vol. 92, 233110, 2008.
27. <http://nano.bsu.by/products/mwcnt>.
28. Shuba, M. V., G. Y. Slepian, S. A. Maksimenko, C. Thomsen, and A. Lakhtakia, "Theory of multiwall carbon nanotubes as waveguides and antennas in the infrared and the visible regimes," *Phys. Rev. B*, Vol. 79, 155403, 2009.